

Physics-based and Machine learning predictions of maneuvering forces in unsteady inflow conditions

MARINE 2021

RODRIGO VILUMBRALES-GARCIA*, GABRIEL D. WEYMOUTH*,[†] AND
BHARATHRAM GANAPATHISUBRAMANI*

*Faculty of Engineering and Physical Science
University of Southampton
Southampton, UK
e-mail: r.vilumbrales-garcia@soton.ac.uk

[†] Data-Centric Engineering Group
Alan Turing Institute
London, UK

ABSTRACT

Multi-vessel coordination and controlled maneuvering through upstream wakes is important to a wide range of marine applications; from surface ships to autonomous underwater vehicles. In this work we study the predictive performance of physics-based and machine-learning (ML) models for unsteady inflow maneuvering forces using tandem flapping foils as a model system. Two physics-based approaches, one following simple quasi-steady assumptions and another that modifies classical Theodorsen, are found to perform fairly well when there are only mild interactions with the upstream wake, with minimum error levels of around 6%. However, this error increases to 40% when there is strong wake interaction. Three ML models were trained and tested; a Long Short-Term Memory (LSTM) model, a Neural Ordinary Differential Equations (NODE) model, and a Sparse Identification of Nonlinear Dynamics (SINDy) approach. We find that all three models can match the low error of the physics-based for mild inflow unsteadiness and are capable of improving the predictions in the case of strong interactions, reducing the error levels below 20%. While these ML models require substantial training data and care in choosing their meta-parameters, their predictions do prove to be more reliable for a wider range of unsteadiness conditions as well as potentially still producing human-interpretable models (in the case of SINDy), making them an interesting research direction for further study.

Keywords: maneuvering; LSTM; Neural ODE; SINDy; Machine Learning; Flapping foils.

1 INTRODUCTION

Multi-vessel coordination and controlled maneuvering through upstream wakes is important to a wide range of marine applications; from surface ships to autonomous underwater vehicles. A proper understanding of the unsteadiness of the surrounding flow is essential, and it is a requirement for safety aspects or to develop operations involving several unmanned vehicles. Previous work has been done in the field of underwater vehicles manoeuvrability [7] and ship-to-ship interactions [22]. In the biological area, studies have found important benefits in terms of travel performance in the case of fish-schooling [19]. What all the previous studies have in common is the importance of properly adapting to the surrounding environment in order to maximise the performance gains and to ensure a safe operation. To replicate this ability of fish to maneuver and take advantage of their unsteady upstream conditions, our engineered vessels need to be able to predict fluid forces in real-time.

As a model problem to study high-speed force predictions, we will investigate the unsteady forces on the back foil of a tandem flapping foil pair. In addition, tandem foils have been suggested for use in

vessel maneuvering because of their high force production capabilities [15]. Several models have been developed to estimate the performance of a flapping foil. Theodorsen and Mutchler [18] derived the first expressions for the forces time evolution to predict aerodynamic flutter. Garrick et al. [5], used the equations defined by Theodorsen to approximate the propulsive forces, and Lighthill [10] completed the work done by Garrick applying its equations to a lunate tail of a fish. The main disadvantage of the previous methods is that they all assume small amplitude kinematic motions, rectilinear vortex wake and perfect fluid, conditions highly unlikely to be found in a real-world applications. A more complex scenario can be found in the tandem flapping foil operation, as one of those two objects is interacting with the wake of the other. If the motion of both bodies is properly tuned, the one in the back can achieve important performance gains. [14] [8]. Muscutt, Weymouth, and Ganapathisubramani [14] predicted the performance of the mentioned hind foil by using a quasi-steady approach, providing accurate results in the cycle-averaged thrust production estimation, but not considering the real-time force signal prediction.

In the recent years, the use of Machine Learning (ML) for control, maneuvering and marine applications has greatly improved. Weymouth and Yue [21] studied the applications of physics-based learning models (PBLM) to ship hydrodynamics. By the use of physical knowledge of the system, the authors improved the predictions obtained by simple regression models at a considerably less expense than high-resolution numerical predictions. Also, several ML tools have been developed for a vast range of applications, from text or image recognition, to forces prediction. Of especial interest for this study are two black-box approaches - where the output is complex and difficult to understand by the user -. The first one is the long short-term memory neural network (LSTM), able to interpret data in a temporal context [6]. By the use of previous system data, LSTM models can predict future states [4] [13]. The second approach is the Neural Ordinary Differential Equations (NODE) [3], that can provide time-series approximation and predictions when the data is irregularly sampled or insufficient [16]. Another ML approach, this time in the “physics-based” ML group, is the Sparse Identification of Nonlinear Dynamical systems (SINDy) [2], where user-interpretable governing equations can be prescribed.

In this study, we analyse several methods in order to develop a model able to estimate the performance of a flapping foil under unsteady upstream conditions. In Section 2, the problem definition is explained. Several flapping foil tandem configurations have been simulated, and the forces and flow conditions faced by the hind foil recorded, to later serve both as inputs for the models and as target. In Section 3, two physics-based approaches, the quasi-steady and Theodorsen models, are adapted in order to include the effects of the unsteadiness of the upstream flow. Next, in Section 4, we develop three Machine Learning models, LSTM, NODE and SINDy. In section 5, we study the capabilities of all five models and evaluate them against data obtained with an in-house CFD software. The predictive performance, in terms of time-signal estimation and prediction error is studied, and the limitations of the models discussed.

2 Problem definition and data generation

Our model problem for maneuvering in unsteady inflow conditions is a tandem foil configuration, Figure 3. We define c as the chord length of the foil, $a = c/4$ is the pivoting point location for the pitching motion, $b = c/2$ is half the chord of the foil, U_∞ is the free-stream velocity and $h(t), \theta(t)$ are the heave and pitch of the foil, defined as

$$h(t) = A \sin(2\pi ft + \phi) \quad (1)$$

$$\theta(t) = \theta_{max} \cos(2\pi ft + \phi) \quad (2)$$

where $A = c$ is the heaving amplitude, f is the flapping frequency, and ϕ represents the phasing in the motion between the two foils. Finally, two other parameters need to be introduced. The first one

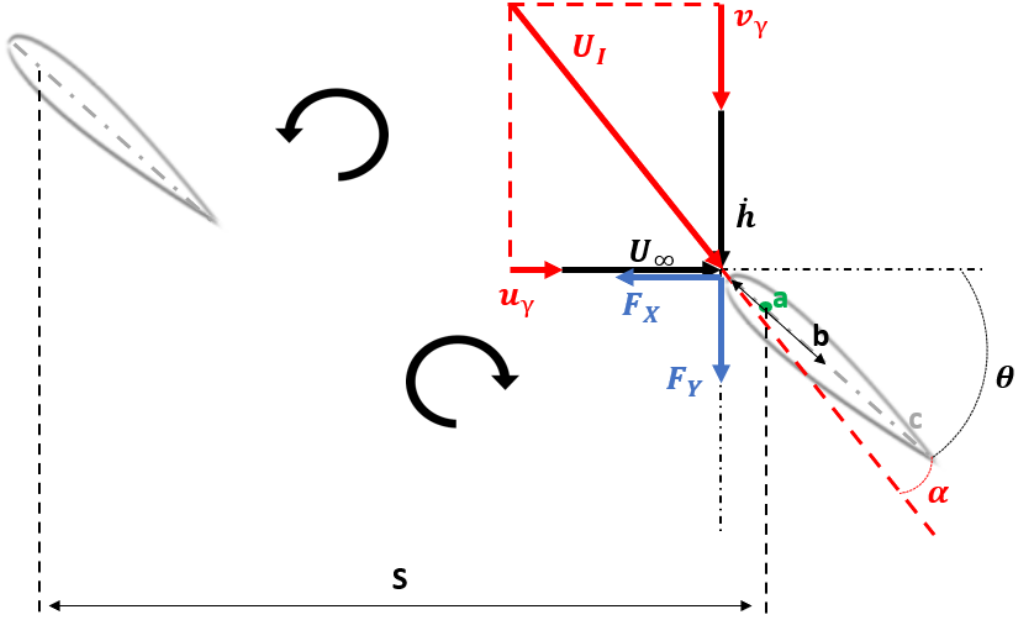


Figure 1. Sketch of the tandem flapping foil system and induced unsteady forces. The rotating arrows indicate the presence of circulation from the upstream foil. The red terms indicate how the upstream unsteadiness influence the effective velocity and angle of attack of the second foil.

is the Strouhal number $St = 2Af/U_\infty$ and the Reynolds number $Re_c = U_\infty c/v$, where v is the fluid kinematic viscosity. In this work we use $Re_c = 7000$ and $St = 0.3 - 0.5$ to match previous tandem foil studies [14].

The effective angle of attack of the back foil α depends on the uniform flow, the heave velocity and on the unsteady inflow conditions produced by the motion of the front foil

$$\alpha = \arctan\left(\frac{-\dot{h} - v_\gamma}{U_\infty + u_\gamma}\right) + \theta \quad (3)$$

where u_γ and v_γ are the horizontal and vertical velocity components induced by the vorticity of the upstream wake.

A range of tandem configurations are tested in order to study the effectiveness of the prediction methods for different foil-wake interactions. The varied parameters are the foils relative phase ϕ and their longitudinal spacing S . As discovered by [14], the combination of the previous parameters will have a strong influence in the performance of the hind foil and two specific setups have been selected as a test cases for the different force prediction approaches. The first one corresponds to a High-Performance hind foil ($St=0.3$, $\phi=1.75\pi$, $S=2.5c$), or a foil able to extract energy from the wake of the leader, and hence to achieve a performance augmentation. The hind foil has minimal interaction with the vortex structures of the fore-foil in this case. The second case is Low-Performance hind foil ($St=0.3$, $\phi=\pi$, $S=2.5c$), where much less thrust is generated because the flow is strongly disrupted by the upstream vortex structures.

An in-house CFD solver is used to generate the benchmark data to study this system. This solver uses the Boundary Data Immersion Method (BDIM,[20]) to simulate the time-evolution of the viscous Navier-Stokes using a convolution over the fluid and any immersed dynamic geometries. The convergence of this method is quadratic, and has been previously validated for flapping foil systems in several studies [12, 9, 23]. A rectangular Cartesian mesh is used with a grid spacing of $\Delta X = \Delta Y = c/192$ near the foils and in the inter-foil region with grid stretching used in the outer fluid domain. This is

Table 1. Numerical cases

St value	0.3, 0.4, 0.5
Spacing	0.5, 1, 1.5, 2, 2.5, 3, 3.5, 4, 4.5, 5
Phasing	$0\pi, 0.25\pi, 0.50\pi, 0.75\pi, 0\pi, 1.25\pi, 1.5\pi, 1.750\pi$
Number of simulations	240 tandem cases

the same gird used and validated in [9].

The CFD method was used to simulate a broad range of test conditions for the model problem defined above, Table 1. For each of the tandem cases, the performance of the hind foil, in terms of the time histories of the force along the x-axis $C_X=2F_X/(\rho U_\infty^2 c)$ and the transverse force $C_Y=2F_Y/(\rho U_\infty^2 c)$, are recorded and used to assess the performance estimation models. In addition, the unsteady "inflow" velocity conditions u_γ, v_γ to the downstream foil are recorded for use in some the maneuvering force models.

3 Physics-based performance estimation approaches

This section covers two theoretical estimations, starting with a simple quasi-steady approach, and progressing towards a more complex model with foundations in Garrick and Theodorsen's analysis. In both methods, the effects of the flow unsteadiness has been introduced via the information gathered about the foil surroundings.

3.1 Quasi-steady model

Following [14], a baseline quasi-steady model for the instantaneous lift on the downstream flapping foil is defined as

$$C_L = -2\pi\alpha \quad (4)$$

where the local α is defined in Equation (3). Projecting this into the horizontal and vertical axis, C_Y and C_X are obtained as

$$C_Y = C_L \cos(\theta - \alpha) \quad (5)$$

$$C_X = C_L \sin(\theta - \alpha) \quad (6)$$

3.2 Adapted Theodorsen model

The second physics-based approach is developed from the work of Theodorsen and Mutchler [18] and Garrick et al. [5] for small amplitude unsteady foil motions. Using the notation presented in Fig. 1, the unsteady lift force a foil in a uniform inflow (such as the upstream foil) is modelled as

$$L = -\rho b^2(U\pi\dot{\theta} + \pi\ddot{h} - \pi b a \ddot{\theta}) - 2\pi\rho U b C(k) \left[U\theta + \dot{h} + b(1/2 - a)\dot{\theta} \right] \quad (7)$$

where Theodorsen's function $C(k)$ is a transfer function relating sinusoidal inputs of reduced frequency to their aerodynamic response [1] [18].

To modify this function for unsteady inflow, we augment the vertical velocity produced by the heaving motion of the body \dot{h} with the velocity induced by the wake along the transverse direction v_γ , and augment the horizontal inflow velocity U with the wake induced velocity u_γ . Combining this with the appropriate values of a, b and using our definition of the effective back foil angle of attack α gives the adapted version of equation 7 for the back foil as

$$C_L = -\frac{c\pi}{2U} \left(\dot{\alpha} + \frac{c\ddot{\theta}}{4U} \right) - 2\pi \left(\alpha + \frac{c\dot{\theta}}{2U} \right) \quad (8)$$

Table 2. Machine Learning models: state vector

$$\mathbf{Z}(\mathbf{t}) = [U(\mathbf{t}), \alpha(\mathbf{t}), \dot{\alpha}(\mathbf{t}), \theta(\mathbf{t}), \dot{\theta}(\mathbf{t}), C_X(\mathbf{t}), C_Y(\mathbf{t})]$$

This value of C_L can then be used to obtain the transverse force using,

$$C_Y = C_L \cos(\theta - \alpha) \quad (9)$$

The propulsive force can be obtained using [5],

$$C_X = C_L \theta + \frac{2\pi S_x^2}{cU^2} \quad (10)$$

Here S_x is the leading-edge suction component developed in [5], and rewritten following the notation presented in Figure 1:

$$S_x = \frac{\sqrt{2}}{2} \left[2C(k)Q - \frac{c\dot{\theta}}{2} \right], \quad \text{where, } Q = U\alpha + \frac{c\dot{\theta}}{2} \quad (11)$$

4 Machine Learning performance estimation approaches

In this section, we study the use of three machine learning models predictions, LSTM, ODE and SINDy, for the C_X and C_Y force coefficients to complement the approximate physical models described above.

Note that the physical parameters used to predict the forces in Eq. 3, 4, 6, and 9 are: the effective angle of attack of the foil, α , the local pitch angle with respect to the x-axis, θ , U , and the derivatives $\dot{\alpha}$, $\dot{\theta}$ and $\ddot{\theta}$. In order to keep simplicity in the ML model, and due to its small contribution to the total forces, the term $\ddot{\theta}$ has been discarded as an input, but the rest, together with C_X and C_Y are used to define the state vector Z for the ML models, see Table 2. Choosing physically-relevant instantaneous flow metrics as the inputs for the ML models should help them generalize to the unseen test cases [21].

4.1 LSTM

The Long Short-Term Memory (LSTM) method, developed by Hochreiter and Schmidhuber [6] is suitable for this analysis as it can pass the information obtained at a given state, or $x(t)$ to the next iteration. By doing so, it can estimate the state of a given parameter at a $(t + \Delta(t))$ time step, what makes the model suitable for predictive - and maneuverability - applications.

The LSTM model, developed using the package Keras [4], is trained using pieces of the time-signal inputs, also known as windows, where the goal is to predict the state of the same inputs, but ahead in time. In this study, 10 time step involving roughly a cycle period $t/T = 0.1$ have been used as an input in order to predict the next $t/T = 0.1$ of the cycle, in a moving prediction until the full cycle is covered. Due to the characteristics of this study, where the goal is to achieve a first approximation to ML for maneuvering applications, no other windows shapes have been considered. Finally, the model takes into account all the variables and combines them in order to obtain the output layer but, as this is essentially a black-box model, the interpretation of the resulting model is not straightforward. Nevertheless, it is important that the network is provided with useful and physics-meaningful data, in order to achieve a result suitable for real applications.

The aim of this part of the study is not to obtain the best-fitted LSTM model with respect to the target data, but to perform a characterisation and sensitivity analysis of the main model parameters. Considering that the number of aspects that can be varied in a LSTM model is vast, only the key

Table 3. LSTM parametric study

Input Layer	$Z(t_0)$, Table 2
LSTM layer	Hidden Units [16,32,64,128,256]
Drop Out layer	DR [0.2,0.5,0.8,No DO]
Output Layer	$Z(t_0 + \Delta t)$, Table 2

Table 4. Neural ODE parametric study

Input Layer	$Z(t_0)$, Table 2
RNN layer (encoder)	Hidden Layer [1], Hidden Units [25]
Latent ODE layer	Hidden Layer [1], Hidden Units [16,32,64,128,256]
Decoder layer	Hidden Layer [1], Hidden Units [20]
Output Layer	$Z(t_0 + \Delta t)$, Table 2

ones have been selected: first, the Hidden Units (HU), and second, the Dropout Rate (DR). Both have been used in other LSTM applications as the network varying parameters [4] [13]. To maintain the model as simple as possible, only one LSTM layer has been used. A summary of the whole model can be seen in the table below:

The combination of the drop out rates and Hidden Units evolves to a total of 20 cases. All of them will be analysed later in the discussion of results, and the best of those in terms of accuracy, will be compared with the findings obtained with the theoretical approach explained earlier in this section. The model has been trained with 160 cases, and tested with two selected cases not seen by the model during the training. All the models use an "adam" optimizer.

4.2 Neural ODE

The Neural Ordinary Differential Equations (NODE) approach, developed by Chen et al. [3] obtains an output layer solution by solving an ODE initial value problem with the use of a black-box differential equation solver.

Neural ODEs are a suitable application for timeseries prediction, especially when the data is irregularly sampled or insufficient [16]. Although that is not the case of our study, where all the time signals are made up of equally-spaced time steps, recent work has proved that it could provide a better estimation to forces signal than the LSTM. Following the work done by [3], an encoder-decoder ODE network has been used in order to predict, like in the LSTM section, the states of several physical parameters ahead of time.

The model has been developed using the package TorchDiffEq [3]. Due to the approach followed on this research, most of the characteristics of the network are kept similar to those presented at [3]. Also, and to keep consistency with the LSTM approach, a sweep in the ODE layer hidden-units has been made. Finally, no dropout layer has been applied, as it has been found that it does not adapt properly to neural ODE networks [11].

4.3 SINDy

The last machine learning method that is going to be used in this study is the Sparse Identification of Nonlinear Dynamics (SINDy) [1]. This approach aims to discover governing equations from measured data and, by assuming that only a few important terms govern those dynamics, SINDy uses sparse regression in order to output user-interpretative models. By doing so, it can overcome one of the

main disadvantages of black box algorithms which, although can provide accurate answers in terms of controlling and maneuvering performance estimation, do not provide a great amount of physical knowledge in return due to the characteristics of their output models.

In this study, the package *PySINDy* [17] has been used. As part of the definition of the model, a second-degree differentiation has been established, together with a third-degree polynomial order as the feature library. In terms of the optimiser, and considering that it is this part where the interpretability of the output models is going to be defined, two different options have been applied. The first one, where the optimizer is a simple Ordinary Least Squares (OLS), and the second one, that uses a LASSO regression ($\alpha = 2$). The next table details both model conditions. The main difference is going to rely in the amount of parameters that conform the model equations, and will be explained in the results sections.

5 RESULTS

This section introduces the results obtained with the methods presented in the previous chapter. As explained in the methodology, the models have been tested against two test cases, one corresponding to a High-Performance hind foil, in which the level of unsteadiness is reasonably low, and another one, a Low-Performance foil where, due to the strong body-wake interactions, the unsteadiness of the flow is considerably higher.

First, the time signal estimation for a full flapping cycle is presented. Due to the predictive approach followed for the LSTM, SINDy and ODE methods, a rolling average has been computed with the evaluations at each of the data points, and is introduced together with the standard deviation. Like so, it can be possible to appreciate whether the average estimation is accurate, but also to ascertain its stability over time. The real - and target - data obtained with Lotus is presented together with the quasi-steady and adapted Theodorsen models, and selected cases of the LSTM, Neural ODE and SINDy parametric sweep.

It is clear from Figure 2 that the quasi-steady approach does not fit properly the evolution of the C_X obtained by Lotus. It is surprising how, even when the time signal clearly differs, the cycle-averaged thrust value would be close to the real estimation, which proves that a correct modelling of cycle-averaged quantities is not sufficient for a maneuvering model. The adapted Theodorsen, on the other hand, seems to collapse between with the CFD results, although it can not model properly the areas of the cycle where the thrust production is negative. As expected, the prediction is considerably more accurate for the HP case than for the LP, as will be seen later in this section.

The LSTM model, Fig 2 a) and b) appears to capture properly the peak thrust value of the HP test case and the drag-generating parts of the cycle. Although LSTM does not augment the accuracy of the Adapted Theodorsen, the results presented here have to be understood as a first approach to ML techniques. It will be the aim of further work to develop a more consistent method. About the LP test case, the LSTM method appears to capture better the sudden peaks appearing in the CFD signal, caused due to the high unsteady interactions between the foil and the upstream flow, improving the predictions of the Adapted Theodorsen. The second conclusion that can be extracted from the LSTM figure is that the stability of the predictions, represented by the confidence intervals, is in line with the mean thrust estimation, and decreases as the complexity of the model increases.

About the Neural ODE model, part c) and d) of Fig. 2, it can be seen how, for the HP and LP case, the NODE approach appears to collapse better with the target data than the quasi-steady approach, and is close to the Theodorsen predictions, although it has not been able to improve the predictions of the LSTM network. In line with the results presented above, the complexity of the LP test case falls outside of what this Neural ODE model can achieve. On the other hand, the stability of the predictions is higher than the LSTM result, especially at the LP test case.

The SINDy output where a LASSO optimizer has been defined is presented at Fig. 2 e) and f).

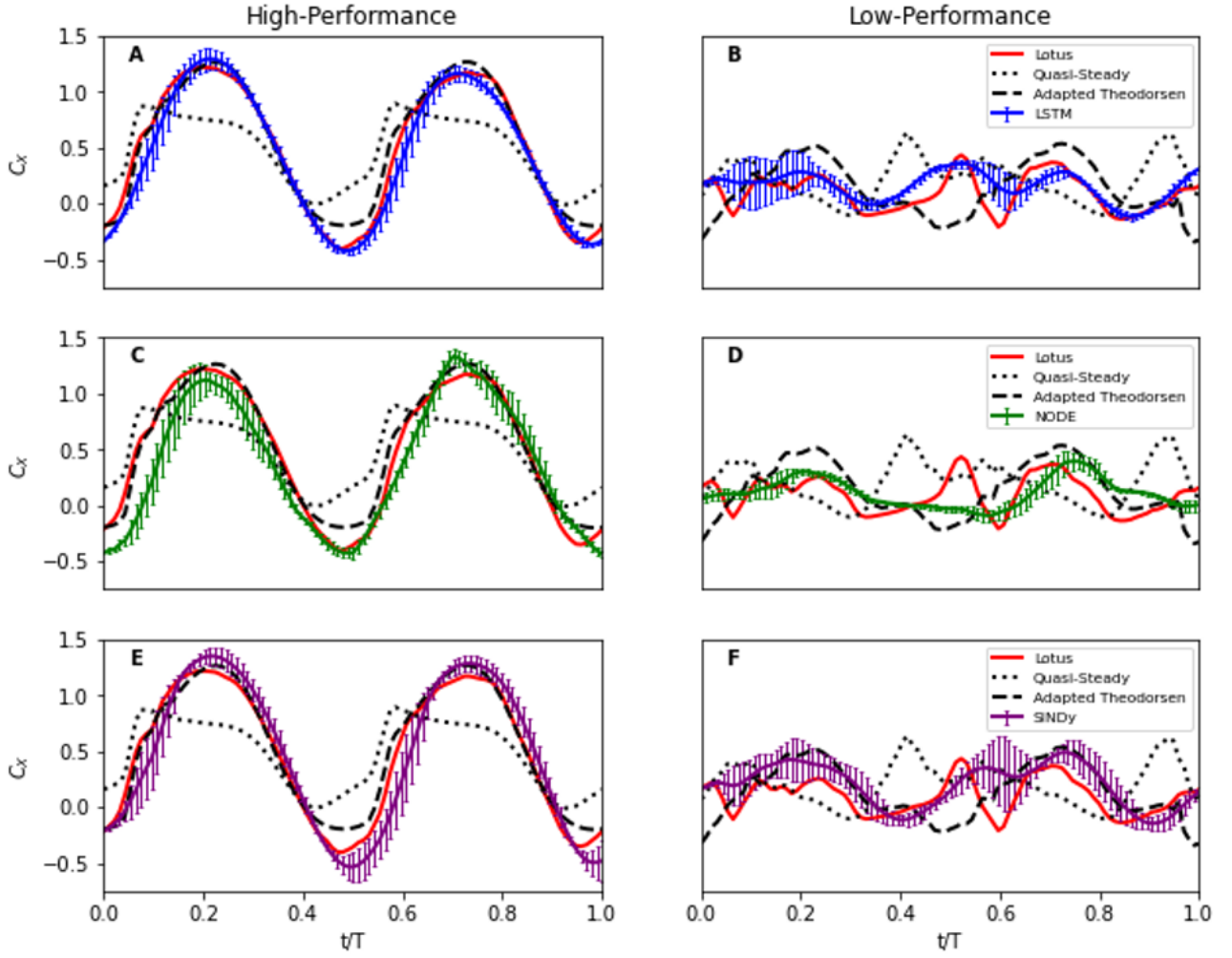


Figure 2. Time signal prediction comparison for the HP case. HP test case at the left column and LP test case at the right column. LSTM results (A and B), NODE results (C and D) and SINDy (LASSO) results (E and F).

Following the trend of the previous LSTM and Neural ODE, the approach performs considerably better than the quasi-steady model, but does not augment the prediction of the adapted Theodorsen, at least for the HP case. The size of the errorbars, indicator of the stability of the predictions, is in line with the LSTM results, and bigger than for the Neural ODE case, especially at the LP case.

Next, in order to evaluate all the methods together, the Normalised Root-Mean-Square Error (NRMSE) is presented. It has been calculated as follows:

$$NRMSE = \frac{RMSE}{y_{max} - y_{min}} \quad (12)$$

Where y_{max} and y_{min} correspond to the maximum and minimum of the Lotus test case C_X and C_Y predictions. The data presented here is the NRMSE result for a full flapping cycle.

As explained before, the methods developed in this study are compared against two test cases, one involving a High-Performance Hind foil, and another representing a Low-Performance scenario. Figure 3 introduces the NRMSE comparison for both cases.

About the quasi-steady and Adapted Theodorsen models, It can be seen in the previous figure how both are obtaining a lower NRMSE for the HP test case than for the LP test. Considering that both theoretical approaches were limited in their original design to a tight range of parameters, especially

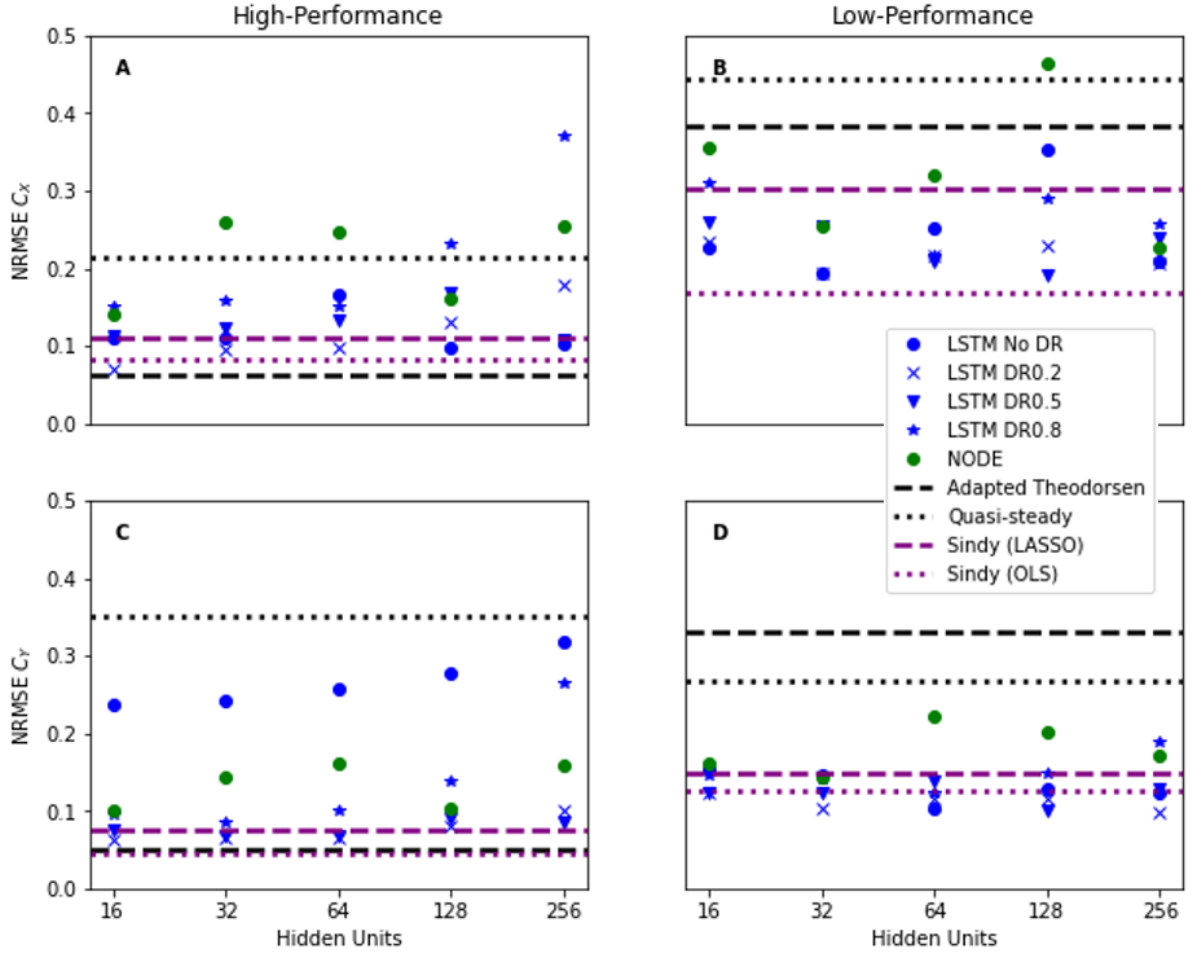


Figure 3. NRMSE comparison. HP test case at the left column and LP test case at the right column. C_X (A and B) and C_Y (C and D)

quasi-steady flow conditions [18] [5], the mentioned result does not come as a surprise. The adapted Theodorsen has been able to obtain, for all the cases but the LP C_Y , a better prediction than the simple quasi steady, especially at the thrust estimation (6% NRMSE error the first one and 21% the second at the HP C_X).

About the LSTM results, and starting with the sensitivity analysis, the amount of Hidden Units (HU) does not appear to have a strong influence in the overall result, although for most of the cases, there is a slight trend indicating that networks with few HU could be beneficial, which could be due to a better dealing with overfitting in the training phase. The Neural ODE approach appears to be less sensitive to the variation of the hidden units than the LSTM.

For the HP test cases, neither the LSTM or the Neural ODE models can increase the accuracy of the adapted Theodorsen. About the LP case, the situation is the opposite, as both LSTM and Neural ODE methods are improving the accuracy of the adapted Theodorsen (originally around 40% error against around 18% for the LSTM and 21% for NODE). Although the ML approaches are not better than the theoretical models - in terms of prediction accuracy - for all scenarios, they can be more stable for a wider range of cases, especially when the unsteadiness increases, what highlights the potential of these methods.

Although it may appear that the OLS SINDy obtains the best prediction, especially at the LP test case (near 17% error), a simple look at the output model can reject it's application. It was explained in the methodology section that the purpose of SINDy was to obtain an interpretable output model, that could lead to knowledge gain about the physics behind the foil-wake interactions but, when using an OLS optimiser, SINDy outputs a C'_X equation with more than 91 parameters. On the other hand,

if a LASSO optimizer is applied, the second SINDy model, the decrease in accuracy is considerably high (especially at the HP), but the amount of terms in the C'_X model goes down to 8.

6 CONCLUSIONS

In this study, several methods have been analysed to develop a high-speed maneuvering model able to estimate the performance of a flapping foil under unsteady upstream conditions. Two physics-based approaches, a simple quasi-steady and a Theodorsen and Garrick approach have been adapted in order to account for the upstream flow unsteadiness. Three machine learning models have been designed and trained, an LSTM, a Neural ODE, and a SINDy model. The physic-based and ML models have been compared against two test cases obtained using full CFD simulations.

While the quasi-steady approach has not provided accurate outputs, the adapted Theodorsen equation has achieved an error of around 6% with respect to the CFD data in the less-complex test case. On the other hand, as the unsteadiness increases, the accuracy quickly goes down, reaching an error of almost 40% for the low performance case.

It was found that both the LSTM and SINDy machine learning could match the accuracy of the adapted Theodorsen for the less-complex test case, the SINDY with 91 parameters achieving 8% error and LSTM achieving around 7% in its best attempt. On the other hand, all the ML models can improve on the accuracy of the adapted Theodorsen in the more unsteady test case, with a best case 20% and 25% error for the LSTM and NODE respectively. The SINDy model is able to reduce the error to only 17% when allowed to use 91 parameters. However, when SINDy with LASSO optimization is used to produce an human-interpretable 8-parameter model, the error jumps up to 30%.

In conclusion, the potential of ML techniques to predict the forces on maneuvering vehicles in unsteady inflow conditions has been demonstrated, especially when the unsteadiness is strong enough to make simple theory-based approaches unreliable. The ML models have proven to be more suitable to be applied for a wider range of conditions than the adapted theoretical approaches, which highlights their potential for maneuverability applications.

Acknowledgments

This research was supported financially by the Office of Naval Research award N62909-18-1-2091. The authors want to acknowledge the support of the University of Southampton's School of Engineering and The Alan Turing Institute.

References

- [1] Steven Brunton and Clarence Rowley. "Modeling the unsteady aerodynamic forces on small-scale wings". In: *47th AIAA aerospace sciences meeting including the new horizons forum and aerospace exposition*. 2009, p. 1127.
- [2] Steven L Brunton, Joshua L Proctor, and J Nathan Kutz. "Discovering governing equations from data by sparse identification of nonlinear dynamical systems". In: *Proceedings of the national academy of sciences* 113.15 (2016), pp. 3932–3937.
- [3] Ricky TQ Chen et al. "Neural ordinary differential equations". In: *arXiv preprint arXiv:1806.07366* (2018).
- [4] Francois Chollet et al. *Deep learning with Python*. Vol. 361. Manning New York, 2018.
- [5] IE Garrick et al. "Propulsion of a flapping and oscillating airfoil". In: *NACA report 567* (1937), pp. 419–427.
- [6] Sepp Hochreiter and Jürgen Schmidhuber. "Long short-term memory". In: *Neural computation* 9.8 (1997), pp. 1735–1780.

- [7] Minsung Kim et al. “Integral sliding mode controller for precise manoeuvring of autonomous underwater vehicle in the presence of unknown environmental disturbances”. In: *International Journal of Control* 88.10 (2015), pp. 2055–2065.
- [8] Melike Kurt and Keith W Moored. “Flow interactions of two-and three-dimensional networked bio-inspired control elements in an in-line arrangement”. In: *Bioinspiration & biomimetics* 13.4 (2018), p. 045002.
- [9] NS Lagopoulos, GD Weymouth, and Bharathram Ganapathisubramani. “Universal scaling law in drag-to-thrust wake transition of flapping foils”. In: *arXiv preprint arXiv:1903.03050* (2019).
- [10] MJ Lighthill. “Hydromechanics of aquatic animal propulsion”. In: *Annual review of fluid mechanics* 1.1 (1969), pp. 413–446.
- [11] Xuanqing Liu et al. “Neural sde: Stabilizing neural ode networks with stochastic noise”. In: *arXiv preprint arXiv:1906.02355* (2019).
- [12] Audrey P Maertens and Gabriel D Weymouth. “Accurate Cartesian-grid simulations of near-body flows at intermediate Reynolds numbers”. In: *Computer Methods in Applied Mechanics and Engineering* 283 (2015), pp. 106–129.
- [13] Arturo Marban et al. “A recurrent convolutional neural network approach for sensorless force estimation in robotic surgery”. In: *Biomedical Signal Processing and Control* 50 (2019), pp. 134–150.
- [14] Luke Muscutt, Gabriel Weymouth, and Bharathram Ganapathisubramani. “Performance augmentation mechanism of in-line tandem flapping foils”. In: *Journal of Fluid Mechanics* (2017), pp. 484–505.
- [15] Douglas A Read, FS Hover, and MS Triantafyllou. “Forces on oscillating foils for propulsion and maneuvering”. In: *Journal of Fluids and Structures* 17.1 (2003), pp. 163–183.
- [16] Yulia Rubanova, Ricky TQ Chen, and David Duvenaud. “Latent ordinary differential equations for irregularly-sampled time series”. In: (2019).
- [17] Brian M de Silva et al. “PySINDy: A Python package for the sparse identification of nonlinear dynamics from data”. In: *arXiv preprint arXiv:2004.08424* (2020).
- [18] Theodore Theodorsen and WH Mutchler. “General theory of aerodynamic instability and the mechanism of flutter”. In: (1935).
- [19] D Weihs. “Hydromechanics of fish schooling”. In: *Nature* 241.5387 (1973), pp. 290–291.
- [20] Gabriel D Weymouth and Dick KP Yue. “Boundary data immersion method for Cartesian-grid simulations of fluid-body interaction problems”. In: *Journal of Computational Physics* 230.16 (2011), pp. 6233–6247.
- [21] GD Weymouth and D. K. P. Yue. “Physics-Based Learning Models for Ship Hydrodynamics”. In: *Journal of Ship Research* 57.1 (Mar. 2013), pp. 1–12.
- [22] Dongchi Yu, Lu Wang, and Ronald W Yeung. “Experimental and numerical study of ship-to-ship interactions in overtaking manoeuvres”. In: *Proceedings of the Royal Society A* 475.2225 (2019), p. 20180748.
- [23] Andhini N Zurman-Nasution, Bharathram Ganapathisubramani, and Gabriel D Weymouth. “Effects of aspect ratio on rolling and twisting foils”. In: *Physical Review Fluids* 6.1 (2021), p. 013101.